JOURNAL OF AIRCRAFT
Vol. 32, No. 4, July–August 1995

Experimental Investigation of Tangential Slot Blowing on a Generic Chined Forebody

Russell M. Cummings*
California Polytechnic State University, San Luis Obispo, California 93407
Lewis B. Schiff†
NASA Ames Research Center, Moffett Field, California 94035
and
John D. Duino‡
California Polytechnic State University, San Luis Obispo, California 93407

An experimental investigation of tangential slot blowing was performed on a generic chined forebody. Low-speed measurements of lateral forces and moments were made on the forebody at high angles of attack (0 deg $\leq \alpha \leq$ 45 deg). Tangential slot blowing was investigated as a means of forebody flow control to generate side force and yawing moment levels capable of overcoming flow asymmetries. The effects of jet mass flow ratio and jet longitudinal position were studied. Limited flowfield visualization was also conducted in order to gain a better understanding of the flowfield characteristics. Tangential slot blowing was found to overcome the natural flow asymmetry of the forebody throughout the angle-of-attack range studied.

Nomenclature

C_m = pitching-moment coefficient, $m/q_\infty S_{ref} d_{ref}$
C_N = normal-force coefficient, $N/q_\infty S_{ref}$
C_n = yawing-moment coefficient, $n/q_\infty S_{ref} d_{ref}$
C_Y = side-force coefficient, $Y/q_\infty S_{ref}$
C_μ = slot-blowing momentum coefficient, $\dot{m}_{slot} V_{slot}/q_\infty S_{ref}$
d_{ref} = reference diameter (cone base diameter), 8.08 in.
MFR = mass flow ratio, $\dot{m}_{slot}/\dot{m}_{ref}$
M_∞ = freestream Mach number, 0.06 (nominal)
m = pitching moment
$\dot{m}_{ref}$ = reference mass flow rate, $\rho_\infty V_\infty S_{ref}$
$\dot{m}_{slot}$ = slot mass flow rate, $\rho_{slot} V_{slot} S_{slot}$
N = normal force
n = yawing moment
q_∞ = freestream dynamic pressure, $\frac{1}{2}\rho_\infty V_\infty^2$; 5.18 lb/ft^2 (nominal)
Re_d = Reynolds number based on reference diameter, $\rho_\infty V_\infty d_{ref}/\mu_\infty$; 2.81 × 10^5 (nominal)
Re_∞ = Reynolds number based on freestream conditions, $\rho_\infty V_\infty/\mu_\infty$; 4.18 × 10^5/ft (nominal)
S_{ref} = reference area (cone base area), 51.276 in.^{2}
S_{slot} = slot area (per slot), 0.005 in.^{2} (nominal)
V_{slot} = jet velocity at the slot exit
V_∞ = freestream velocity, 66.7 ft/s (nominal)
Y = side force
α = angle of attack
β = angle of sideslip
ΔC_n/MFR = jet blowing efficiency
μ_∞ = freestream coefficient of viscosity
ρ_{slot} = jet density at the slot exit
ρ_∞ = freestream air density

Introduction

FUTURE aircraft designs will make use of the fixed separation points of chined forebodies, as evidenced by the YF-22 configuration. Wind-tunnel tests[1] show that a chined forebody produces more lift than a conventional circular cross-section forebody, even at poststall angles of attack. This is due to the additional planform area and the suction produced by the strong forebody vortices. The high-angle-of-attack characteristics of these forebodies has been studied and found to be favorable,[2,3] with improved lateral-directional stability due to the strong forebody vortices originating at the fixed separation line.[4,5]

As the flight envelope of present and future aircraft continues to expand and includes the high-angle-of-attack flight regime, there is a need to understand the complex flowfield about aircraft flying in this regime. The flowfield about an aircraft at large incidence is dominated by large regions of three-dimensional separated flow, where the boundary layer separates from the body and rolls up on the leeward side of the body to form strong vortices.[6,7] This separated flow reduces the effectiveness of the aircraft control systems, such as rudders, and makes it increasingly difficult for the aircraft to be controlled (Fig. 1).

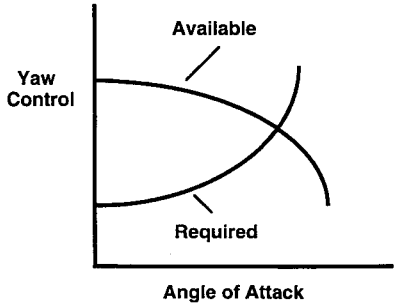

Fig. 1 Yaw control power.

Received July 18, 1994; presented as Paper 94-3477 at the AIAA Atmospheric Flight Mechanics Conference, Scottsdale, AZ, Aug. 1–3, 1994; revision received Feb. 8, 1995; accepted for publication Feb. 10, 1995.

*Professor and Chairman, Aeronautical Engineering Department. Associate Fellow AIAA.
†Special Assistant for High Alpha Technology. Associate Fellow AIAA.
‡Graduate Research Assistant, Aeronautical Engineering Department; currently Member of the Technical Staff, North American Aircraft Division, Rockwell International, El Segundo, CA 90245. Member AIAA.

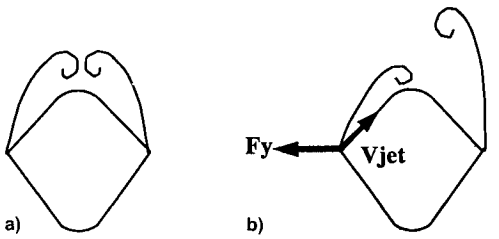

Fig. 2 Effects of tangential slot blowing: a) no-blowing and b) blowing from the top surface.

One of the concepts being looked at for augmenting control of aircraft flying at high angles of attack is forebody flow control. There are several methods being researched that can provide forebody flow control, including mechanical and pneumatic methods (experiments and numerical investigations have shown that both methods are feasible[8,9]). Forebody tangential slot blowing has been shown to be a candidate for forebody flow control, which is accomplished by blowing a thin sheet of air tangentially to the forebody surface from a slot, as shown in Fig. 2.[10] The blowing causes the forebody vortices to change positions in the vicinity of the aircraft and alters the side force and yawing moment. The pilot can use the blowing to control the aircraft while flying at high angles of attack.

A small-scale wind-tunnel experiment was performed in the California Polytechnic State University (Cal Poly) 3 × 4 ft low-speed wind tunnel to study the effectiveness of tangential slot blowing for forebody flow control on a generic chined forebody and a cone forebody. In the experiment, the forces and moments acting on the forebody were measured while the jet mass flow rate, slot length, and forebody angle of attack were varied. A companion computational investigation has also been performed[11] in order to determine the effects of varying jet mass flow rate, angle of attack, and blowing slot location on the chined forebody flowfield. These investigations have shown that tangential slot blowing is a viable and efficient method for forebody flow control, and that the blowing is most efficient when done near the tip of the nose. A description of the results of the experiment follows.

Experimental Apparatus

The wind-tunnel test was conducted for both a circular cone and a generic chined forebody. Both models were 20.25 in. in length and approximately 8.0 in. in diameter at the base. The chined forebody had a shape as shown in Fig. 3, with blowing slots located on the upper surface of the chine. The slots began approximately 0.5 in. from the tip of the nose and ran for 5.0 in. on both the port and starboard sides of the model. The slots were subdivided into 1.0-in. segments so that various blowing slot lengths could be tested. The slots were designated as being either port P or starboard S (as viewed from the base). The slots blew air tangentially to the forebody surface within the crossflow plane, as shown in Fig. 2 (the cone model only had slots on the port side). The slot segments are nominally 1.0 in. in length and 0.005 in. in width, with the forward-most segment being labeled no. 1, the next most forward segment being labeled no. 2, etc., and the final segment being labeled no. 5. Each slot segment had a small plenum chamber controlled by valves located outside of the wind tunnel and was capable of producing various amounts of blowing. Pressurized air was provided at 100 psi to the valve control panel, and the valves were connected to the slots through tubing that ran along the sting and through the base of the model.

The models were tested in the Cal Poly 3 × 4 ft low-speed wind tunnel. Installation photographs of the chined forebody in the test section are presented in Figs. 4 and 5. The tunnel is capable of producing test section velocities ranging from 10

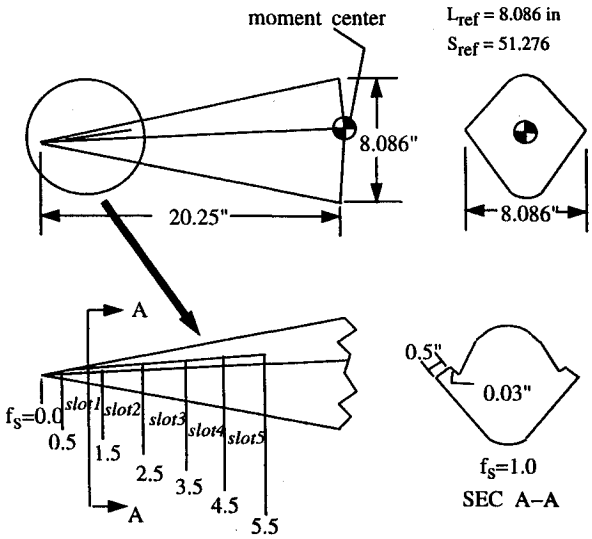

Fig. 3 Wind-tunnel model dimensions.

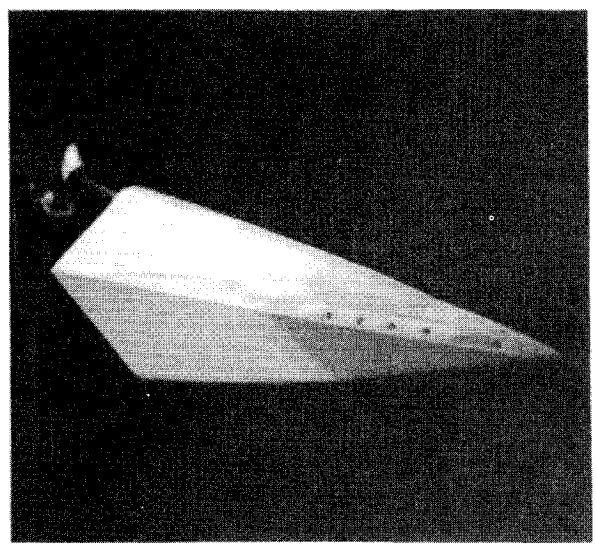

Fig. 4 Generic chined forebody installed at α = 0 deg.

to 30 m/s. The test section is fitted with an Aerolab six-component sting and balance system. The electrical inputs from the balance system are directly fed into a Hewlett Packard Model 3421A Data Acquisition/Control Unit for computing forces and moments. The data acquisition unit sampled 50 force and moment measurements, which were averaged in order to eliminate any small unsteadiness. The yawing-moment coefficient data have an accuracy of ±3%.

The model/sting installation used for this test was capable of producing angles of attack ranging from α = 0 to 45 deg. The majority of experimental data was obtained for test section velocities of V_∞ = 66.0 ft/s, which corresponds to a free-stream Reynolds number of Re_∞ = 4.18 × 10^5/ft, or a Reynolds number based on model diameter of Re_d = 2.81 × 10^5.

The models were tested for a variety of slot lengths. First, individual segments were tested throughout the angle-of-attack range with various amounts of slot blowing. Combinations of segments were then tested in order to determine which slot, or combination of slots produced the most efficient results. Runs were also made at sideslip angles of β = 5 and −5 deg, with many of the slot segment combinations being tested again for these conditions.

A light sheet was utilized to obtain flowfield smoke flow visualizations. The visualizations could be used to determine the movements of the vortices as the slot blowing was in-

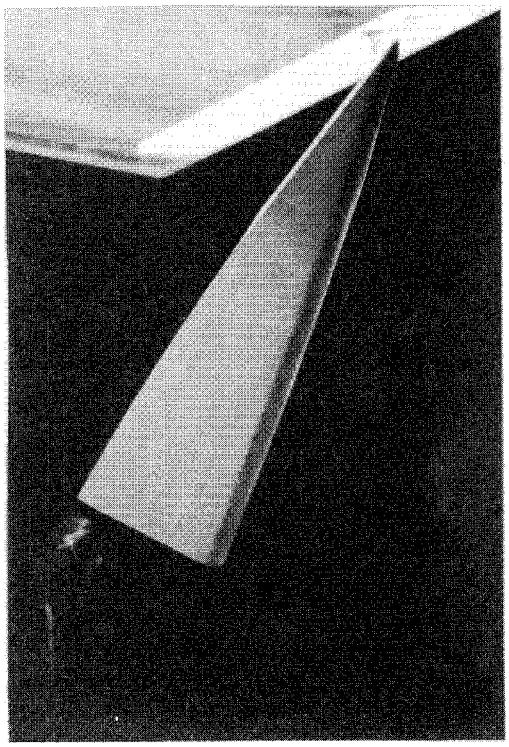

Fig. 5 Generic chined forebody installed at $\alpha = 45$ deg.

creased or decreased. The light was provided by a high voltage arc lamp fitted with a double-slot mechanism to focus a sheet of light across the wind-tunnel test section. A smoke wand with a thin wire probe was used to seed the flow upstream of the forebody model. Every attempt was made to minimize the effect of the smoke wand on the flowfield characteristics.

Experimental Results

The main purpose of the wind-tunnel experiment was to determine whether tangential slot blowing could overcome the natural asymmetric vortex patterns that are created in the flowfield about a body at high angles of attack. Further, if blowing could overcome the asymmetries, the study was to investigate the levels of blowing required to control the vortex position. In this way an aircraft control system would be feasible that utilizes tangential slot blowing as a control method.

The data presented were all taken at a freestream velocity of $V_\infty = 66.0$ ft/s and at nominal blowing volume flow rates Q (in units of standard cubic feet per hour, ft^3/h), ranging from $0 \leq Q$ (ft^3/h) ≤ 60. These volume flow rates correspond to MFRs ranging from $0 \leq$ MFR ≤ 0.00148 and blowing coefficients C_μ ranging from $0 \leq C_\mu \leq 0.0502$. Table 1 presents a calibration of volume flow rate, mass flow rate, mass flow ratio, and blowing coefficient for this test. The angles of attack range from 0 deg $\leq \alpha \leq 45$ deg (the reference line for $\alpha = 0$ deg was chosen to be the chine). The majority of the data are presented in terms of incremental yawing-moment coefficients, where the incremental coefficients are defined to be $\Delta C_n = C_n(\text{MFR} \neq 0) - C_n(\text{MFR} = 0)$, which provides the effectiveness of the blowing at any single freestream condition. No flowfield unsteadiness was observed during the experiment except at $\alpha = 45$ deg.

Longitudinal characteristics for the generic chined forebody with and without blowing are presented in Figs. 6 and 7. Figure 6 shows the normal-force coefficient and Fig. 7 shows the pitching-moment coefficient, both as a function of angle of attack. The blowing cases are for the maximum mass flow ratio of MFR = 0.00148. As can be seen for both the pitching-moment and normal-force coefficients, the blowing had negligible effects on the longitudinal characteristics throughout the angle-of-attack range.

Table 1 Calibration of flow rates

Q, ft^3/h	$\dot{m}_{slot}$, lb/s	MFR	C_μ
10	1.74E-04	9.62E-05	0.0002
20	4.16E-04	2.31E-04	0.0014
30	7.22E-04	4.02E-04	0.0041
40	1.22E-03	6.78E-04	0.023
50	1.90E-03	1.06E-03	0.0358
60	2.67E-03	1.48E-03	0.0502
80	4.31E-03	2.39E-03	0.0811
120	7.60E-03	4.22E-03	0.1431

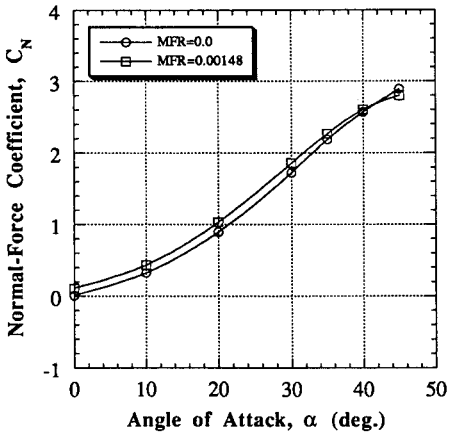

Fig. 6 Normal-force coefficient variation with angle of attack.

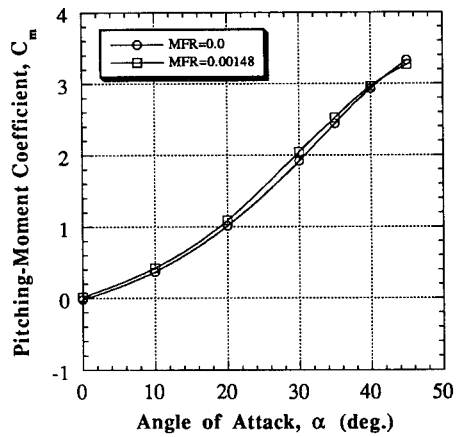

Fig. 7 Pitching-moment coefficient variation with angle of attack.

Although a great deal of data were collected for both the cone and chined forebodies, only chined forebody data will be presented in this article. In addition, only yawing-moment coefficient data will be shown to illustrate the aerodynamic characteristics of tangential slot blowing. The side-force coefficient data show similar trends and lead to the same conclusions.

The variation with angle of attack of the incremental yawing-moment coefficients due to blowing from the starboard slots with various fixed mass flow ratios are presented in Fig. 8. Blowing at the lowest rate (MFR = 0.000231), as shown in Fig. 8a, does not produce any appreciable effects on the yawing moment (as a matter of comparison, the maximum magnitude for the coefficient without blowing is $|C_n| \leq 0.06$). The effectiveness of the slot blowing is beginning to be seen at MFR = 0.00678 (Fig. 8b). At this mass flow ratio, the yawing-moment coefficients for the forward-most slot (slot no. 1) are significantly larger than the natural yawing moment

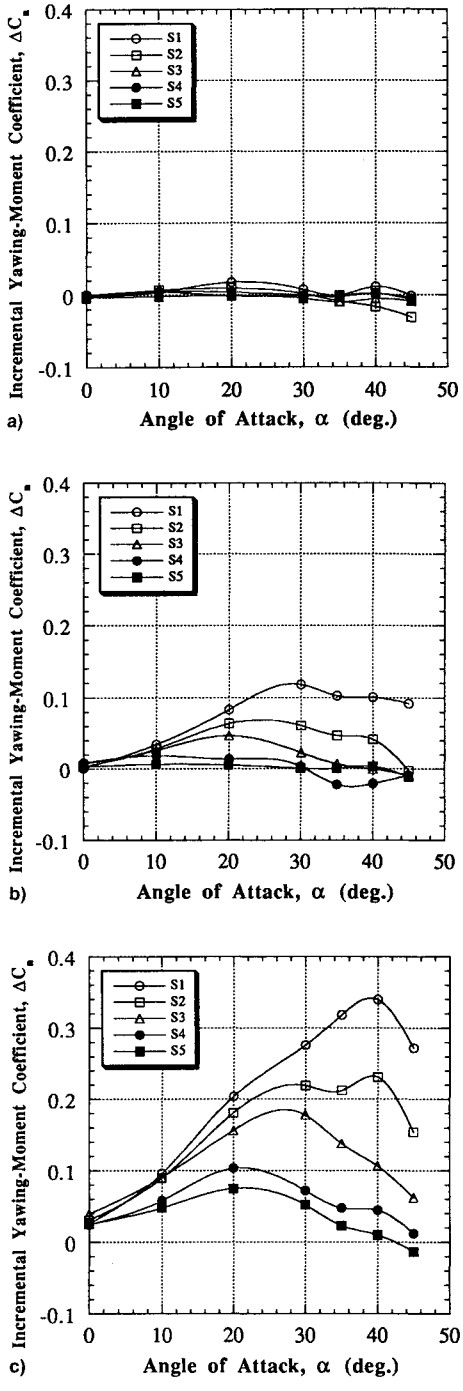

Fig. 8 Effect of starboard slot blowing on yawing-moment coefficient: MFR = a) 0.000231, b) 0.000678, and c) 0.001480.

of the configuration. Figure 8c shows the yawing-moment coefficient for MFR = 0.00148, where the overall trend is becoming clear. The blowing rate is sufficiently high to control the lateral-directional characteristics of the configuration, but only for blowing at the forward-most slot. As the blowing is done from the slots more aft on the forebody (slot nos. 2–5), the effectiveness decreases nearly continuously. Nearly the same results are obtained for blowing from the port slots at MFR = 0.00148 (Fig. 9). More detailed data for port slot blowing can be found in Ref. 12.

Results obtained for blowing from multiple slots on the starboard side of the body are presented in Fig. 10. This plot compares blowing from the first three slots individually at MFR = 0.00148, with blowing from two slots at a total MFR = 0.00422 (various combinations of slot segments are shown),

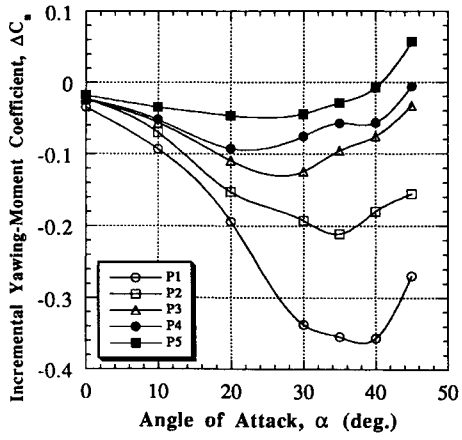

Fig. 9 Effect of port slot blowing on yawing-moment coefficient, MFR = 0.00148.

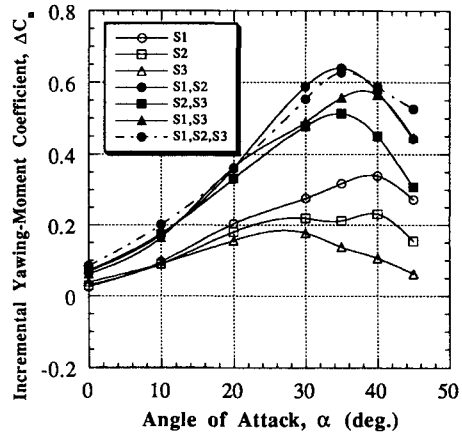

Fig. 10 Effect of single- and multiple-starboard slot blowing on yawing moment (single-slot MFR = 0.001480, double slot MFR = 0.004220, triple slot MFR = 0.006800); starboard and port slot blowing.

and blowing from all three slots at a total MFR = 0.00680. This represents an equal mass flow rate from each slot segment regardless of the slot configuration. As was true for the single-slot blowing case, a general trend is evident: the further forward the slot, the more effective the blowing. This seems to hold true whether the slot is blowing alone or in combination with other more rearward slots. This shows that blowing from multiple slots can produce greater yawing-moment coefficient magnitudes, but not necessarily more efficiently.

The relative effectiveness of blowing from multiple slots is more clearly seen in Fig. 11, where the effects of single- and multiple-slot blowing on yawing moments are shown as a function of mass flow ratio for four angles of attack. Data for α = 30, 35, 40, and 45 deg are shown in Figs. 11a–11d, respectively. The data for the single-slot blowing cases (slot no. 1) includes three mass flow ratios, while the multiple slot cases only have a single mass flow ratio. These figures show that a single forward slot will produce a desired level of yawing moment coefficient for smaller amounts of mass flow ratio than any of the multiple slot combinations. By far, the greatest efficiency (blowing efficiency is defined as ΔC_n/MFR) is obtained by blowing from the most forward single slot. Figure 12 presents the blowing efficiency that is approximated for these cases (and for the lower angles of attack as well). These approximations are made from the available data in Fig. 11 and should not be construed to be highly accurate, but a definite qualitative trend is apparent. The most forward single slot produces more yawing moment for a given amount of mass flow ratio than do the multiple slot configurations.

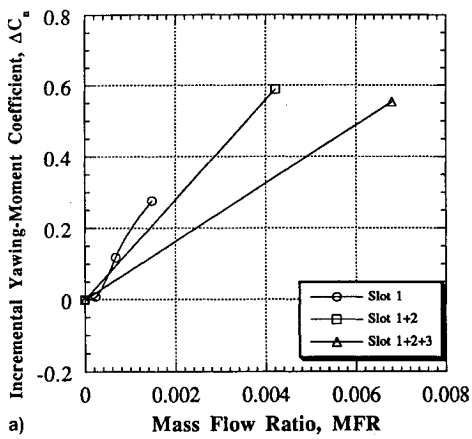

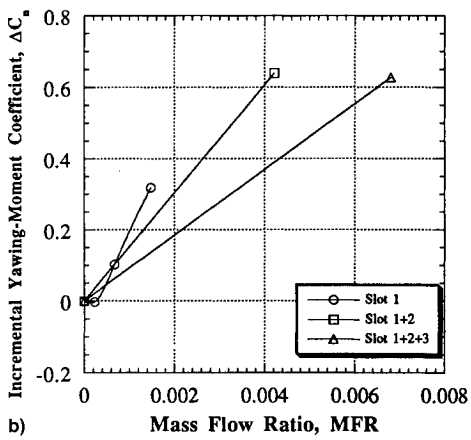

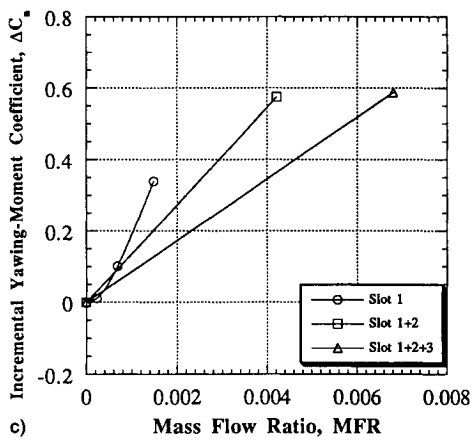

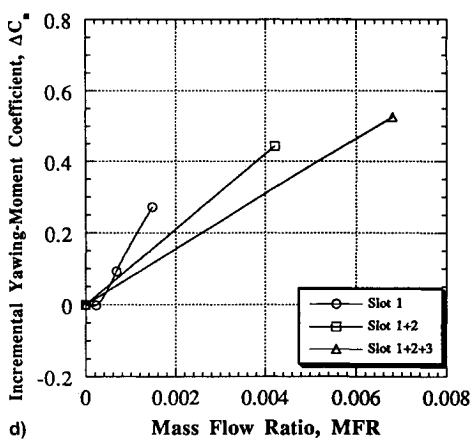

Fig. 11 Multiple slot blowing at various angles of attack: α = a) 30, b) 35, c) 40, and d) 45 deg.

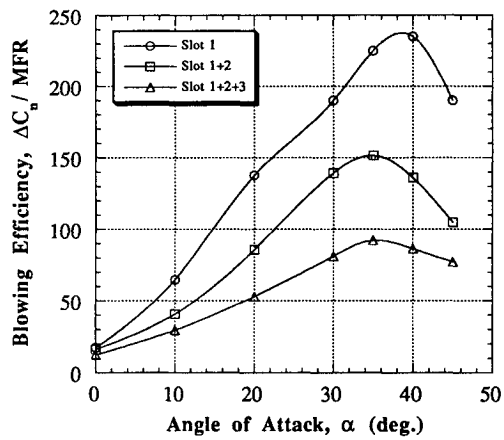

Fig. 12 Blowing efficiency for multiple slots.

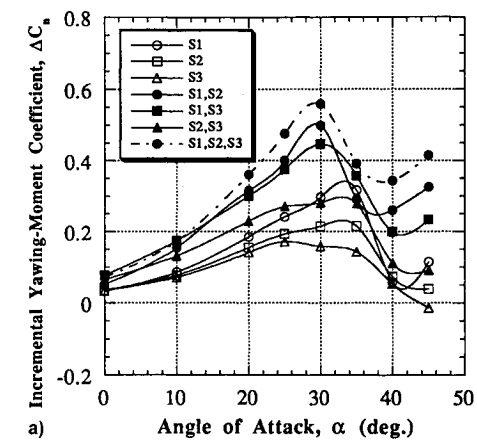

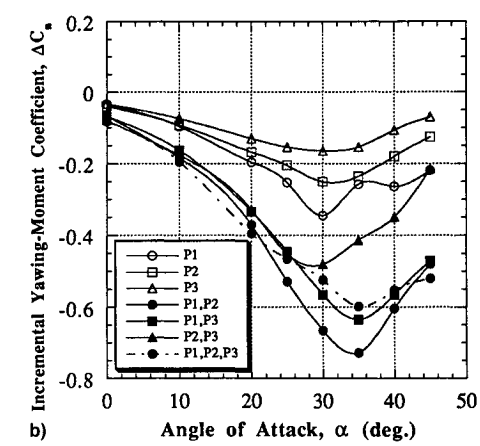

Fig. 13 Comparison of single and multiple segment blowing with the body at sideslip; β = +5 deg (single-slot MFR = 0.001480, double-slot MFR = 0.004220, triple-slot MFR = 0.006800): a) starboard and b) port slot blowing.

Data were also measured for blowing with the forebody at angles of sideslip. Both β = 5 and −5 deg were tested, with blowing from both starboard and port slots. Figure 13 shows the effectiveness for single- and multiple-segment slot blowing for both the starboard and port slots with the forebody at positive angle of sideslip β = 5 deg. Results for β = −5 deg are analogous and may be found in Ref. 12. Again, this data shows that blowing from a single-slot segment at the front of the chine is most efficient.

The ability of single-slot blowing to overcome the yawing moment due to sideslip of the chined forebody is presented

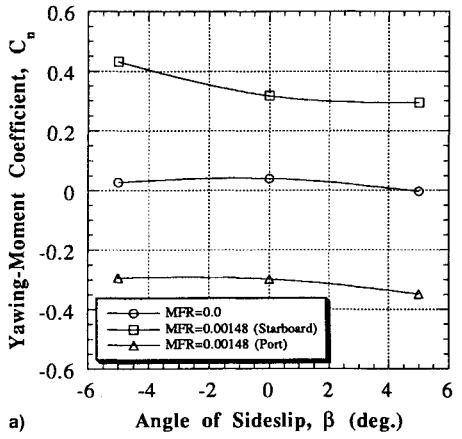

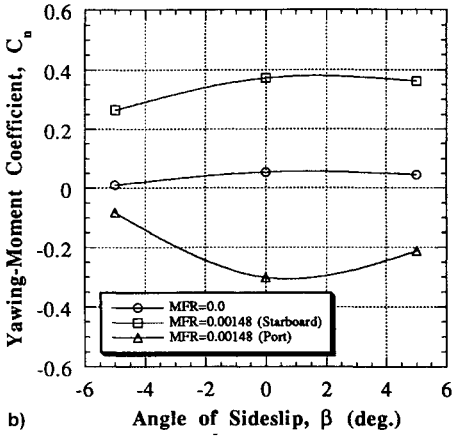

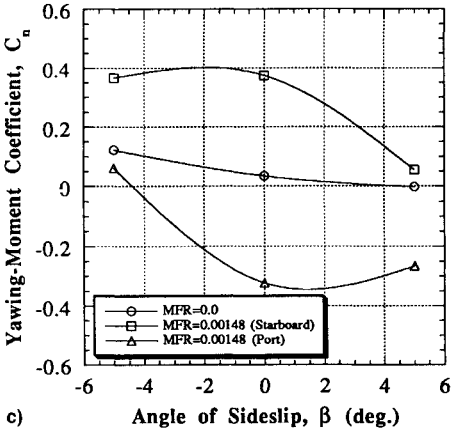

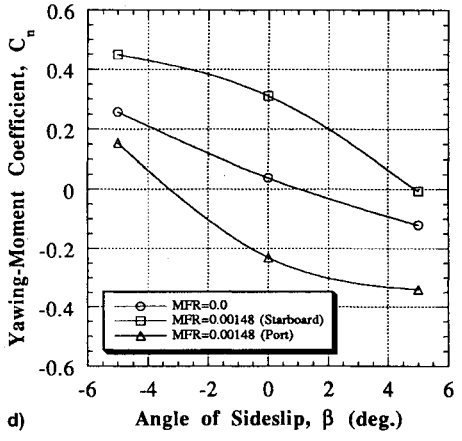

Fig. 14 Ability of single-slot blowing to overcome yawing moment, $\beta = 0, \pm 5$ deg: α = a) 30, b) 35, c) 40, and d) 45 deg.

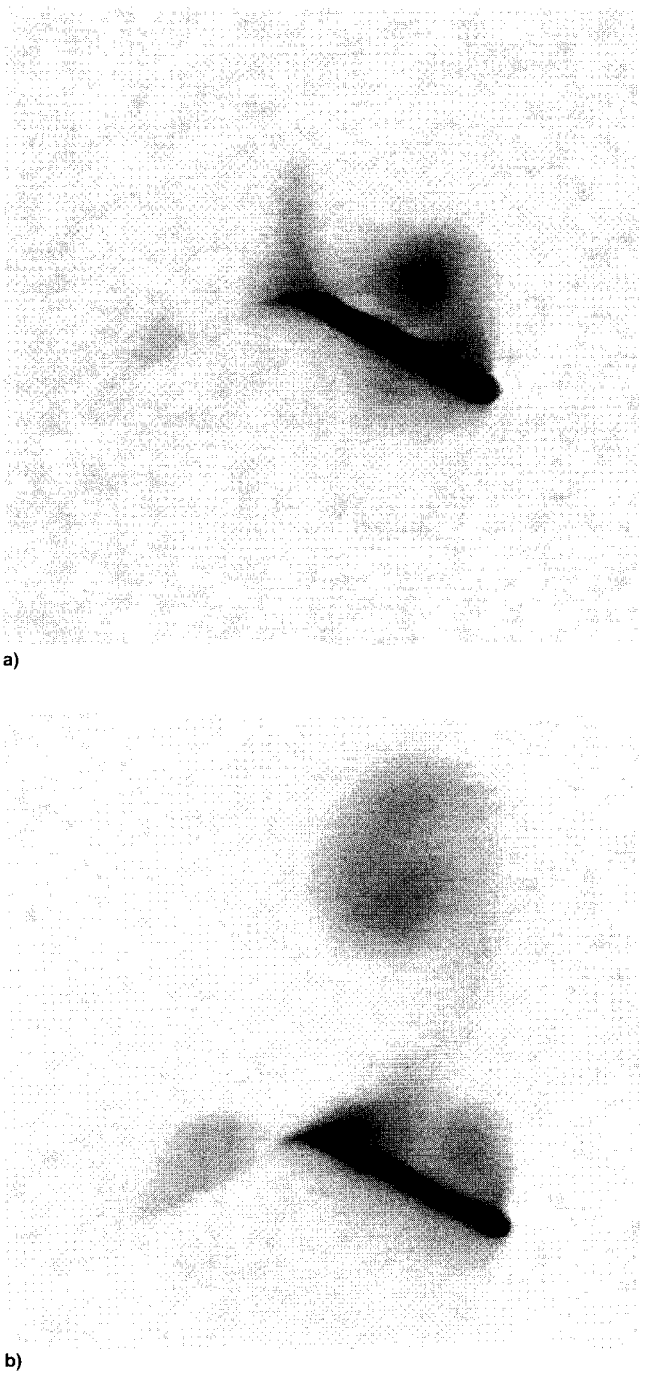

Fig. 15 Light sheet negative flow visualization, $\alpha = 40$ deg: a) no blowing and b) maximum blowing.

in Fig. 14. Data for $\alpha = 30$, 35, 40, and 45 deg are shown in Figs. 14a–14d, respectively. In general, the data show that the single forward slot blowing at MFR = 0.00148 can overcome the yawing moments of the forebody throughout the angle-of-attack and angle of sideslip range tested. For example, the data for $\alpha = 30$ deg (Fig. 14a) shows that the yawing moment produced by either the starboard or port blowing can easily overcome the "natural" yawing moment of the forebody. A few exceptions to this general observation can be seen at the highest angles of attack tested. At $\alpha = 45$ deg and $\beta = -5$ deg (Fig. 14d) the yawing moment due to blowing does not overcome the natural yawing moment; additional mass flow rate would have to be utilized for this case in order to control the forebody.

In general, the changes due to blowing from the starboard slot at positive sideslip are equivalent to those due to blowing

from the port slot at negative sideslip (and vice versa), as seen in Figs. 14a, 14c, and 14d. However, a discrepancy is apparent for $\alpha = 35$ deg (Fig. 14b), where the yawing moment for starboard blowing at $\beta = 5$ deg does not closely match the value for port blowing at $\beta = -5$ deg. This is probably due to slight irregularities in the model and/or wind tunnel, in conjunction with the fact that the incremental yawing moments due to blowing are undergoing a sharp decrease near $\alpha = 35$ deg. Figure 13a shows this effect. At $\alpha = 40$ and 45 deg, the incremental yawing moments are less sensitive to small changes in angle of attack, and the symmetry of the incremental yawing moments is re-established (Figs. 14c and 14d).

A light sheet and smoke wand were used to obtain a limited amount of flow visualization videos at the highest angles of attack. A light sheet negative for $\alpha = 40$ deg, with and without blowing, is shown in Fig. 15. Figure 15a shows the starboard vortex for the no-blowing case; blowing from the port slot results in the vortex pattern shown in Fig. 15b. As the blowing rate is increased, the starboard vortex interacts with the blowing flowfield and creates a new combined starboard vortex pattern (Fig. 15b). This vortex is located significantly higher above the forebody than the no-blowing vortex. The ability of the blowing to take advantage of the Coanda effect over the top of the forebody, and to interact with the starboard vortex, allows for the creation of a variety of flow patterns, and thus, a variety of yawing-moment coefficients throughout the angle-of-attack range.

Conclusions

Experimental data from a low-speed wind-tunnel test have been presented for a chined forebody with tangential slot blowing. The data show that the blowing is able to overcome the natural vortex asymmetries at high angles of attack. Furthermore, the data show that blowing from slots closest to the nose of the forebody is more effective than blowing from slot positions further aft. This slot position effectiveness is valid at various blowing rates and for blowing from single or multiple slots. Test data also shows that slot blowing is able to overcome asymmetries due to moderate sideslip angles. The data presented show that tangential slot blowing is an effective way to overcome vortex asymmetries at high angles of attack.

Acknowledgments

This research was supported by NASA Joint Research Interchange NCA2-626. The contributions of the many students at Cal Poly who made the completion of this research project possible is greatly appreciated: Roxana Agosta, Jaime Alvarez, Amanda Hendrix, Donovan Mathias, Monty Moshier, John Riley, Michael Seelos, David Smario, Deanne Trigs, and John Williams.

References

[1]Boalbey, R. E., Ely, W., and Hahne, D. E., "High Angle of Attack Stability and Control Concepts for Supersonic Fighters," *High-Angle-of-Attack Technology*, NASA CP-3149, 1992, pp. 759–784.

[2]Roos, F. W., and Kegelman, J. T., "Aerodynamic Characteristics of Three Generic Forebodies at High Angles of Attack," AIAA Paper 91-275, Jan. 1991.

[3]Ravi, R., and Mason, W. H., "A Computational Study on Directional Stability of Chine-Shaped Forebodies at High-α," AIAA Paper 92-30, Jan. 1992.

[4]Erickson, G. E., and Brandon, J. M., "Low-Speed Experimental Study of the Vortex Flow Effects of a Fighter Forebody Having Unconventional Cross-Section," AIAA Paper 85-1798, Aug. 1985.

[5]Erickson, G. E., "On the Non-Linear Aerodynamics and Stability Characteristics of a Generic Chine-Forebody Slender-Wing Fighter Configuration," AIAA Paper 87-2617, Aug. 1987.

[6]Schiff, L. B., Cummings, R. M., Sorenson, R. L., and Rizk, Y. M., "Numerical Simulation of High-Incidence Flow over the Isolated F-18 Fuselage Forebody," *Journal of Aircraft*, Vol. 28, No. 10, 1991, pp. 609–617.

[7]Gee, K., Cummings, R. M., and Schiff, L. B., "Turbulence Model Effects on Separated Flow About a Prolate Spheroid," *AIAA Journal*, Vol. 30, No. 3, 1992, pp. 655–664.

[8]Ng, T. T., and Malcolm, G. N., "Aerodynamic Control Using Forebody Strakes," AIAA Paper 91-618, Jan. 1991.

[9]Malcolm, G. N., Ng, T. T., and Lewis, L., "Development of Non-Conventional Control Methods for High Angle of Attack Flight Using Vortex Manipulators," AIAA Paper 89-2192, July 1989.

[10]Gee, K., Rizk, Y. M., Murman, S. M., Lanser, W. R., Meyn, L. A., and Schiff, L. B., "Analysis of a Pneumatic Forebody Flow Control Concept About a Full Aircraft Geometry," AIAA Paper 92-2678, June 1992.

[11]Agosta-Greenman, R. M., Gee, K., Schiff, L. B., and Cummings, R. M., "Numerical Analysis of Tangential Slot Blowing on a Generic Chined Forebody," AIAA Paper 94-3475, Aug. 1994.

[12]Cummings, R. M., Schiff, L. B., and Duino, J. D., "Experimental Investigation of Tangential Slot Blowing on a Generic Chined Forebody," AIAA Paper 94-3477, Aug. 1994.